

Master's thesis

Draft report

v1.3

April 3, 2009

F.A. Klaver

University of Twente
Department of Applied Mathematics

Contents

1	Introduction	1
2	Mathematical models	2
2.1	Introduction	2
2.2	Linear potential flow model	2
2.2.1	Variational formulation	4
2.2.2	Analytical solutions	6
2.3	Shallow water model	9
2.3.1	Variational formulation	10
2.4	Coupling of the models	12
2.5	Conclusion	14
3	Numerical methods	15
3.1	Introduction	15
3.2	Linear potential flow model	15
3.2.1	Harmonic waves	15
3.2.2	Linear waves generated by a wave maker	15
3.3	Shallow water model	16
3.3.1	Riemann problem	17
3.3.2	Burgers' solution	17
3.4	Coupling of the models	18
3.4.1	Verification	18
3.5	Conclusion	19
4	Experimental validation	20
4.1	Introduction	20
4.2	Experimental data	20
4.3	Numerical simulation	20
4.4	Conclusion	20
5	Conclusions and recommendations	21
5.1	Introduction	21
5.2	Conclusions	21
5.2.1	Recommendations for MARIN	21
5.2.2	Future research	21

1 Introduction

The Maritime Research Institute Netherlands (MARIN) facilitates a basin where offshore models are tested in a realistic environment (source: MARIN site). In this Offshore Basin waves are generated using wave makers. In order to prevent reflected waves from interfering with the waves in the basin, passive wave absorbers are installed opposite to the wave makers. The current computational models at MARIN describing the waves in the Offshore Basin do not incorporate the simulation of the fluid at these wave absorbers. The goal of this research is to develop a numerical model of the surface waves in the Offshore Basin included simulating of the behaviour of the fluid at the passive wave absorbers. The approach used in the research is the coupling of a linear potential flow model with a shallow water model. The linear potential flow model that is used is developed by Ambati/Bokhove (more?) and describes surface waves in a incompressible, irrotational fluid when no wave breaking is present. The shallow water model describing the wave motion at the wave absorbers can handle these breaking waves. In chapter 2 the mathematical model is described. Chapter 3 involves the presentation of the numerical methods that are used for the simulation of water waves in the Offshore Basin. The numerical results for each of the two models are compared with exact solutions. In chapter 4 simulation are compared with real data of the Offshore Basin. This report ends with conclusions and recommendations which can be found in chapter 5.

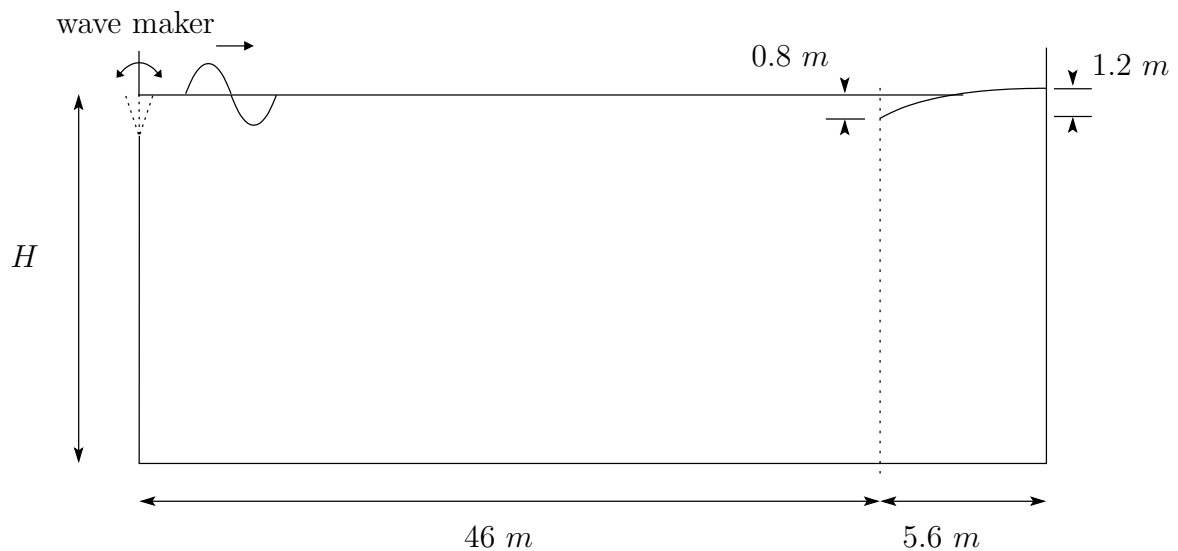


Figure 1: Sketch of the wave tank

2 Mathematical models

2.1 Introduction

In this chapter the mathematical models that describe the wave motion in the Offshore Basin (OB) are presented. As can be seen from the side view sketch of the OB in figure 1 (chapter 1), the OB consists of a deep water part and a shallow water part, the latter being located at the wave absorbers at the right end of the domain. The wave motion in the OB is described by a linear potential flow model for the deep water part and a one dimensional depth-averaged shallow water model for the shallow water part. A sketch of the modeled domain is depicted in figure 2, with domain I being the deep water domain and domain II the shallow water domain. In the next two sections (sections 2.2 and 2.3) each of these models are treated. In section 2.4 the coupling of these two models is treated.

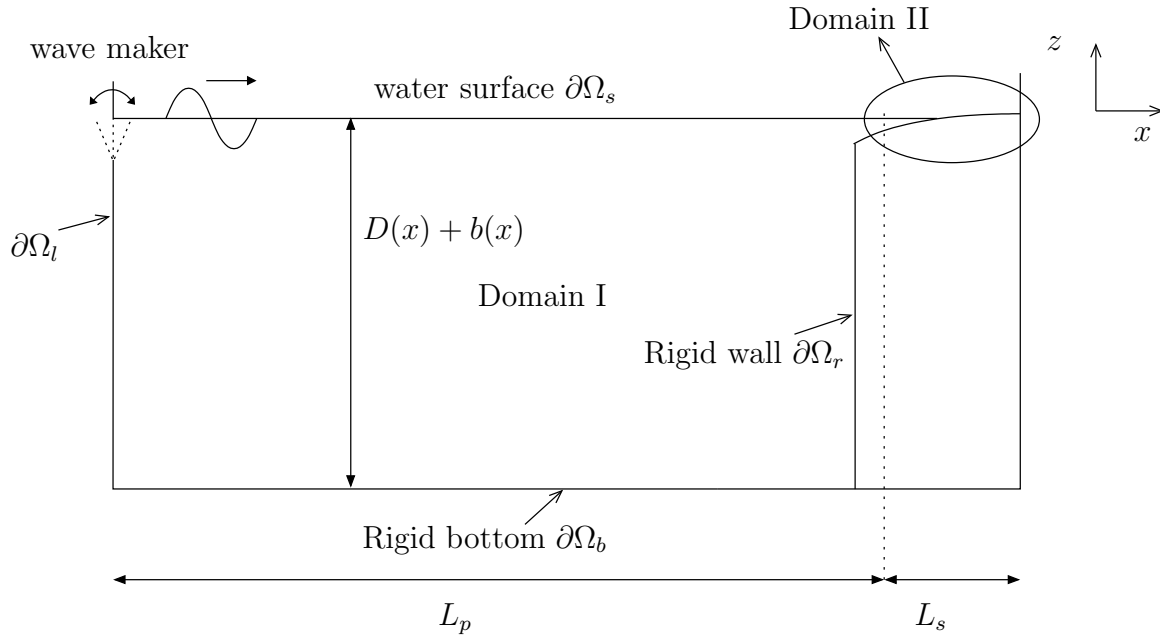


Figure 2: Domain of consideration

2.2 Linear potential flow model

The wave motion in the deep water part of the OB is described by a linear potential flow model. The domain under consideration is shown in figure 2. The linear potential model for this domain is given by Laplace's equation

$$-\nabla^2\Phi = 0 \text{ in } \Omega, \quad (2.1)$$

combined with boundary conditions. At the free surface $\partial\Omega_S$ the following boundary conditions apply:

$$\partial_t\Phi + g\eta = 0 \text{ and} \quad (2.2)$$

$$\partial_t\eta - \partial_z\Phi = 0. \quad (2.3)$$

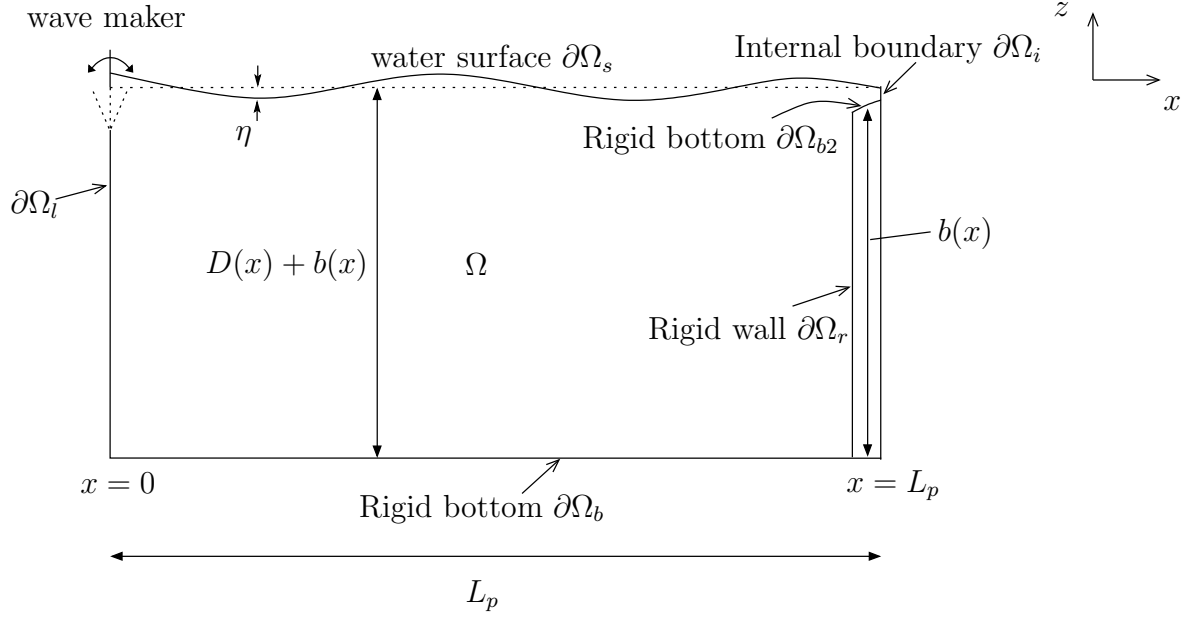


Figure 3: Potential flow domain (domain I)

The boundaries $\partial\Omega_b$, $\partial\Omega_r$ and $\partial\Omega_{b_2}$ are modeled as fixed impermeable walls, therefore a no normal flow boundary condition applies on both of these boundaries:

$$\begin{aligned} \mathbf{n}_b \cdot \nabla \Phi &= 0 \quad \text{on } \partial\Omega_b, \\ -\mathbf{n}_r \cdot \nabla \Phi &= 0 \quad \text{on } \partial\Omega_r, \\ \mathbf{n}_{b_2} \cdot \nabla \Phi &= 0 \quad \text{on } \partial\Omega_{b_2}. \end{aligned}$$

Because of the flat (horizontal) bottom at $\partial\Omega_b$ and the vertical wall at $\partial\Omega_r$ the boundary conditions reduce to:

$$\partial_z \Phi = 0 \quad \text{on } \partial\Omega_b, \quad (2.4)$$

$$-\partial_x \Phi = 0 \quad \text{on } \partial\Omega_r, \quad (2.5)$$

$$\mathbf{n}_{b_2} \cdot \nabla \Phi = 0 \quad \text{on } \partial\Omega_{b_2}. \quad (2.6)$$

The boundary $\partial\Omega_i$ is the boundary that is linked to the shallow water model. The condition for this boundary is derived in section 2.4. In this section it is treated as a fixed impermeable vertical wall:

$$\partial_x \Phi = 0 \quad \text{on } \partial\Omega_i. \quad (2.7)$$

At the left boundary, $\partial\Omega_l$, the wave maker is located, which is modeled as a prescribed horizontal velocity at this boundary (Westhuis):

$$\partial_x \Phi = g(z)T(t) \quad \text{on } \partial\Omega_l. \quad (2.8)$$

The type of wave maker is governed by the function $g(z)$, which is defined as (Schaffer (1996))

$$g(z) = \begin{cases} 1 + \frac{z}{h+l} & \text{for } -(h-d) \leq z \leq 0, \\ 0 & \text{for } -h \leq z \leq -(h-d). \end{cases} \quad (2.9)$$

where l is the length of the wave board, $z = -(h+l)$ is the center of rotation of the board and $d > 0$ the elevation of the rotation point over the bottom of the domain. The wave maker in the OB at MARIN is a flap-type wave maker, which is a hinged board that oscillates around a rotation point (see Westhuis p 86). This type of wave maker corresponds to the case where $l = -d$ (see figure 4), with $l = 1.2m$.

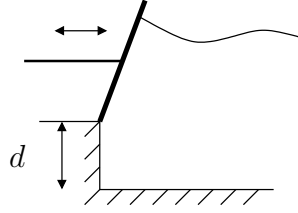


Figure 4: MARIN flap-type wave board

$$\begin{aligned} \nabla^2 \Phi &= 0 & \text{in } \Omega, \\ -\partial_t \Phi - g\eta &= 0 & \text{on } \partial\Omega_s, \\ \partial_t \eta - \nabla \Phi \cdot n_s &= 0 & \text{on } \partial\Omega_s, \\ \partial_z \Phi &= 0 & \text{on } \partial\Omega_b, \\ \partial_x \Phi &= g(z)T(t) & \text{on } \partial\Omega_l, \\ -\partial_x \Phi &= 0 & \text{on } \partial\Omega_r, \\ -\nabla \Phi \cdot n_{b2} &= 0 & \text{on } \partial\Omega_{b2}, \\ -\partial_x \Phi &= 0 & \text{on } \partial\Omega_i. \end{aligned}$$

assumptions: irrotational, incompressible, inviscid flow

2.2.1 Variational formulation

The Lagrangian functional for the modeling of linear potential flow is stated as:

$$\mathcal{L}(\Phi, \eta) = \int_{t_0}^{t_1} \int_{\Omega} -\frac{1}{2} |\nabla \Phi|^2 \, dx \, dz \, dt + \int_{t_0}^{t_1} \int_{\partial\Omega_s} \left\{ -\frac{1}{2} g\eta^2 + \Phi \partial_t \eta \right\} \, dx \, dt, \quad (2.10)$$

with $\Phi = \Phi(x, z, t)$ and $z = \eta(x, t)$ for the case of two-dimensional potential flow.

The equations of motion can be obtained by determining the critical point(s) of the Lagrangian, using the first variation around Φ and η ,

$$\delta \mathcal{L}(\Phi + \varepsilon \delta \Phi, \eta + \varepsilon \delta \eta) = \left. \frac{d}{d\varepsilon} \mathcal{L}(\Phi + \varepsilon \delta \Phi, \eta + \varepsilon \delta \eta) \right|_{\varepsilon=0} = 0, \quad (2.11)$$

Writing (2.11) out:

$$\begin{aligned}
\delta\mathcal{L}(\Phi + \varepsilon\delta\Phi, \eta + \varepsilon\delta\eta) &= \frac{d}{d\varepsilon}\mathcal{L}(\Phi + \varepsilon\delta\Phi, \eta + \varepsilon\delta\eta)\Big|_{\varepsilon=0} = \\
&= \frac{d}{d\varepsilon} \int_{t_0}^{t_1} \int_{\Omega} -\frac{1}{2}|\nabla(\Phi + \varepsilon\delta\Phi)|^2 dx dz dt + \\
&\quad + \int_{t_0}^{t_1} \int_{\partial\Omega_s} \left\{ -\frac{1}{2}g(\eta + \varepsilon\delta\eta)^2 + (\Phi + \varepsilon\delta\Phi)\partial_t(\eta + \varepsilon\delta\eta) \right\} dx dt \Big|_{\varepsilon=0} = \\
&= \frac{d}{d\varepsilon} \int_{t_0}^{t_1} \int_{\Omega} -\frac{1}{2}|\nabla(\Phi + \varepsilon\delta\Phi)|^2 dx dz dt + \\
&\quad + \int_{t_0}^{t_1} \int_{\partial\Omega_s} \left\{ -\frac{1}{2}g(\eta^2 + 2\varepsilon\eta\delta\eta + \varepsilon^2(\delta\eta)^2) + \Phi\partial_t\eta + \Phi\varepsilon\partial_t(\delta\eta) + \varepsilon\delta\Phi\partial_t\eta + \varepsilon^2\delta\Phi\partial_t(\delta\eta) \right\} dx dt \Big|_{\varepsilon=0} = \\
&= \int_{t_0}^{t_1} \int_{\Omega} -|\nabla\Phi| \cdot |\nabla(\delta\Phi)| dx dz dt + \int_{t_0}^{t_1} \int_{\partial\Omega_s} \left\{ -g\eta\delta\eta + \Phi\partial_t(\delta\eta) + \delta\Phi\partial_t\eta \right\} dx dz dt = \\
&= \int_{t_0}^{t_1} \int_{\Omega} \left(-\nabla \cdot (\delta\Phi\nabla\Phi) + \delta\Phi\nabla \cdot (\nabla\Phi) \right) dx dz dt + \int_{t_0}^{t_1} \int_{\partial\Omega_s} \left\{ -g\eta\delta\eta + \Phi\partial_t(\delta\eta) + \delta\Phi\partial_t\eta \right\} dx dz dt = 0
\end{aligned}$$

Applying Gauss' divergence theorem to the first term and integrating the fourth term by parts with respect to t gives:

$$\begin{aligned}
&= \int_{t_0}^{t_1} \int_{\Omega} \delta\Phi\nabla \cdot (\nabla\Phi) dx dz dt + \int_{t_0}^{t_1} \int_{\partial\Omega_s} (-\partial_t\Phi(\delta\eta) + (\delta\Phi)\partial_t\eta - g\eta(\delta\eta)) dx dz dt + \int_{\partial\Omega_s} [\Phi\delta\eta]_{t_0}^{t_1} dx + \\
&\quad + \int_{t_0}^{t_1} \int_{\partial\Omega_s} -(\delta\Phi)\nabla\Phi \cdot n_s dx dz dt + \int_{t_0}^{t_1} \int_{\partial\Omega_b} -(\delta\Phi)\nabla\Phi \cdot n_b dx dy dt + \int_{t_0}^{t_1} \int_{\partial\Omega_l} -(\delta\Phi)\nabla\Phi \cdot n_l dz dt + \\
&\quad + \int_{t_0}^{t_1} \int_{\partial\Omega_r} -(\delta\Phi)\nabla\Phi \cdot n_r dz dt + \int_{t_0}^{t_1} \int_{\partial\Omega_{b2}} -(\delta\Phi)\nabla\Phi \cdot n_{b2} dz dt + \int_{t_0}^{t_1} \int_{\partial\Omega_i} -(\delta\Phi)\nabla\Phi \cdot n_I dz dt = \\
&= \int_{t_0}^{t_1} \int_{\Omega} (\delta\Phi)(\nabla^2\Phi) dx dz dt + \int_{t_0}^{t_1} \int_{\partial\Omega_s} (\delta\eta)(-\partial_t\Phi - g\eta) + (\delta\Phi)(\partial_t\eta - \nabla\Phi \cdot n_s) dx dz dt + \\
&\quad + \int_{\partial\Omega_s} [\Phi\delta\eta]_{t_0}^{t_1} dx + \int_{t_0}^{t_1} \int_{\partial\Omega_b} (\delta\Phi)(-\partial_x\Phi) dx dz dt + \int_{t_0}^{t_1} \int_{\partial\Omega_l} (\delta\Phi)(\partial_x\Phi) dz dt + \\
&\quad + \int_{t_0}^{t_1} \int_{\partial\Omega_r} (\delta\Phi)(-\partial_x\Phi) dz dt + \int_{t_0}^{t_1} \int_{\partial\Omega_{b2}} (\delta\Phi)(-\nabla\Phi \cdot n_{b2}) dz dt + \int_{t_0}^{t_1} \int_{\partial\Omega_i} (\delta\Phi)(-\partial_x\Phi) dz dt = 0
\end{aligned}$$

Because we are considering only domain I in the paragraph, we take the internal boundary $\partial\Omega_i$ to be a fixed wall. Then because $\delta\eta$ and $\delta\Phi$ are zero at $x = 0$, $x = L_p$, $t = t_0$, $t = t_1$ and because of the arbitrariness of $\delta\eta$ and $\delta\Phi$, this results in:

$$\begin{aligned}
\nabla^2\Phi &= 0 && \text{in } \Omega, \\
-\partial_t\Phi - g\eta &= 0 && \text{on } \partial\Omega_s, \\
\partial_t\eta - \nabla\Phi \cdot n_s &= 0 && \text{on } \partial\Omega_s, \\
\partial_z\Phi &= 0 && \text{on } \partial\Omega_b, \\
\partial_x\Phi &= 0 && \text{on } \partial\Omega_l, \\
-\partial_x\Phi &= 0 && \text{on } \partial\Omega_r, \\
-\nabla\Phi \cdot n_{b2} &= 0 && \text{on } \partial\Omega_{b2}, \\
-\partial_x\Phi &= 0 && \text{on } \partial\Omega_i.
\end{aligned}$$

2.2.2 Analytical solutions

For the potential flow model (2.1)-(2.8) analytical solutions can be obtained. Suppose the solution is of the form

$$\Phi(x, z, t) = \hat{\Phi}(x, z)e^{i\omega t} \quad (2.12)$$

Then because of (2.1) we have on Ω :

$$\nabla^2(\hat{\Phi}(x, z)e^{i\omega t}) = 0,$$

or

$$\hat{\Phi}_{xx}e^{i\omega t} + \hat{\Phi}_{zz}e^{i\omega t} = 0,$$

so

$$\nabla^2\hat{\Phi}(x, z) = 0. \quad (2.13)$$

Boundary conditions (2.2) and (2.3) on $\partial\Omega_S$ can be written as a single boundary condition, by differentiating (2.2) with respect to t and substituting (2.3) into (2.2), resulting in:

$$\partial_{tt}\Phi - g\partial_z\Phi = 0 \text{ on } \partial\Omega_S. \quad (2.14)$$

Putting (2.12) into the free surface boundary condition (2.14) gives

$$i^2\omega^2\hat{\Phi}e^{i\omega t} + g\partial_z\hat{\Phi}e^{i\omega t} = 0 \text{ on } \partial\Omega_S,$$

or

$$e^{i\omega t}(g\partial_z\hat{\Phi} - \omega^2\hat{\Phi}) = 0 \text{ on } \partial\Omega_S,$$

resulting in

$$g\partial_z\hat{\Phi} - \omega^2\hat{\Phi} = 0 \text{ on } \partial\Omega_S. \quad (2.15)$$

Substituting (2.12) in (2.8) leads to:

$$\partial_z \hat{\Phi} e^{i\omega t} = 0 \text{ on } \partial\Omega_b,$$

or

$$\partial_z \hat{\Phi} = 0 \text{ on } \partial\Omega_b, \quad (2.16)$$

Now we apply the method of separation of variables for (2.13), (2.15) and (2.16).

Suppose

$$\hat{\Phi}(x, z) = f(x)h(z),$$

Then because of (2.13) we have on Ω :

$$\nabla^2(\hat{\Phi}(x, z)) = \nabla^2(f(x)h(z)) = 0,$$

or

$$\frac{\partial^2 f}{\partial x^2} h + \frac{\partial^2 h}{\partial z^2} f = 0$$

Deviding by fh gives:

$$\frac{\partial^2 h}{\partial z^2} \frac{1}{h} + \frac{\partial^2 f}{\partial x^2} \frac{1}{f}.$$

Because $\frac{\partial^2 h}{\partial z^2} \frac{1}{h}$ depends only on z and $\frac{\partial^2 f}{\partial x^2} \frac{1}{f}$ only on x , we have:

$$\frac{\partial^2 h}{\partial z^2} \frac{1}{h} = k^2 \text{ and } \frac{\partial^2 f}{\partial x^2} \frac{1}{f} = -k^2, \text{ with } k \text{ a constant.}$$

Shorter notated as:

$$f'' = -k^2 f \text{ and } h'' = k^2 h, \text{ with } k \text{ a constant.} \quad (2.17)$$

Boundary condition (2.15) (at the free surface $\partial\Omega_S$) then becomes:

$$gf \partial_z h - \omega^2 fh = 0 \text{ on } \partial\Omega_S,$$

or

$$f(g \partial_z h - \omega^2 h) = 0 \text{ on } \partial\Omega_S.$$

Because $f \neq 0$ (trivial solutions not allowed):

$$g \partial_z h - \omega^2 h = 0 \text{ on } \partial\Omega_S. \quad (2.18)$$

Boundary condition (2.16) then becomes:

$$f \partial_z h = 0 \text{ on } \partial\Omega_b,$$

because $f \neq 0$:

$$\partial_z h = 0 \text{ on } \partial\Omega_b. \quad (2.19)$$

Take $f(x) = e^{-ikx}$ and $h(z) = e^{kz}$, then (2.17) holds. Substituting these in (2.18) gives:

$$gke^{kz} - \omega^2 e^{kz} = 0 \text{ on } \partial\Omega_S \text{ or at } z = 0,$$

or

$$gke^0 - \omega^2 e^0 = 0,$$

or

$$gk - \omega^2 = 0,$$

so

$$\omega = \sqrt{gk}.$$

Substitution of $f(x)$ and $g(z)$ in (2.19) gives:

$$ke^{kz} = 0 \text{ on } \partial\Omega_b \text{ or at } z = -H,$$

or

$$ke^{-kH} = 0,$$

and because $k = 0$ results in $\hat{\Phi} = 1$, we take $h(z) = e^{k(z+H)} + e^{-k(z+H)}$, then (2.19) becomes

$$ke^{k(z+H)} - ke^{-k(z+H)} = 0 \text{ at } z = -H,$$

or

$$ke^0 - ke^0 = 0,$$

so (2.19) holds. With the new f and h boundary condition (2.18) gives:

$$gke^{k(z+H)} - gke^{-k(z+H)} - \omega^2 (e^{k(z+H)} + e^{-k(z+H)}) = 0 \text{ at } z = 0,$$

or

$$gke^{kH} - gke^{-kH} - \omega^2 (e^{kH} + e^{-kH}) = 0,$$

or

$$\omega^2 (e^{kH} + e^{-kH}) = gk (e^{kH} - e^{-kH}),$$

so

$$\omega^2 = \frac{gk(e^{kH} - e^{-kH})}{(e^{kH} + e^{-kH})} = gk \frac{2 \sinh kH}{2 \cosh kH} = gk \tanh kH \quad \text{or} \quad \omega = \sqrt{gk \tanh kH}.$$

Summerizing, we have $f(x) = e^{-ikx}$ and $h(z) = e^{k(z+H)} + e^{-k(z+H)} = 2 \cosh k(z+H)$, resulting in

$$\Phi(x, z, t) = \hat{\Phi}(x, z) e^{i\omega t} = f(x) h(z) e^{i\omega t} = 2 \cosh (k(z+H)) e^{-ikx} e^{i\omega t} = \quad (2.20)$$

$$= 2 \cosh (k(z+H)) e^{i(\omega t - kx)} = A \cosh (k(z+H)) e^{i(\omega t - kx)}. \quad (2.21)$$

Analytical solutions for certain boundary conditions and initial conditions, with and without wave maker.

2.3 Shallow water model

The modeling of the offshore basin at MARIN considered in this report consists of a shallow water part and a deep water part. In the previous section a potential flow model for the deep water part was treated. In this section the shallow water part is presented. This section begins with a description of the mathematical model and gives analytical solutions for some cases. Subsequently ...

The wave run-up in the shallow water part of the domain is modeled by the shallow water equations. The quasi-linear formulation of the shallow water equations in one spatial dimension is given by:

$$\frac{\partial u}{\partial t} + u \frac{\partial u}{\partial x} + g \frac{\partial h}{\partial x} = -g \frac{\partial b}{\partial x}, \quad (2.22)$$

$$\frac{\partial h}{\partial t} + \frac{\partial(hu)}{\partial x} = 0, \quad (2.23)$$

where $h(x, t)$ is the depth of the fluid, $u(x, t)$ the velocity, $g = 9.81m/s^2$ the acceleration of gravity and $b(x)$ the topography defined from a certain reference level. The term $-g \frac{\partial b}{\partial x}$ in the first equation is the source term.

The domain of consideration is $x \in (L_p, L_p + L_s)$, see Figure 5 for a sketch of the domain, with $h(x, t) = D(x, t) + b(x)$.

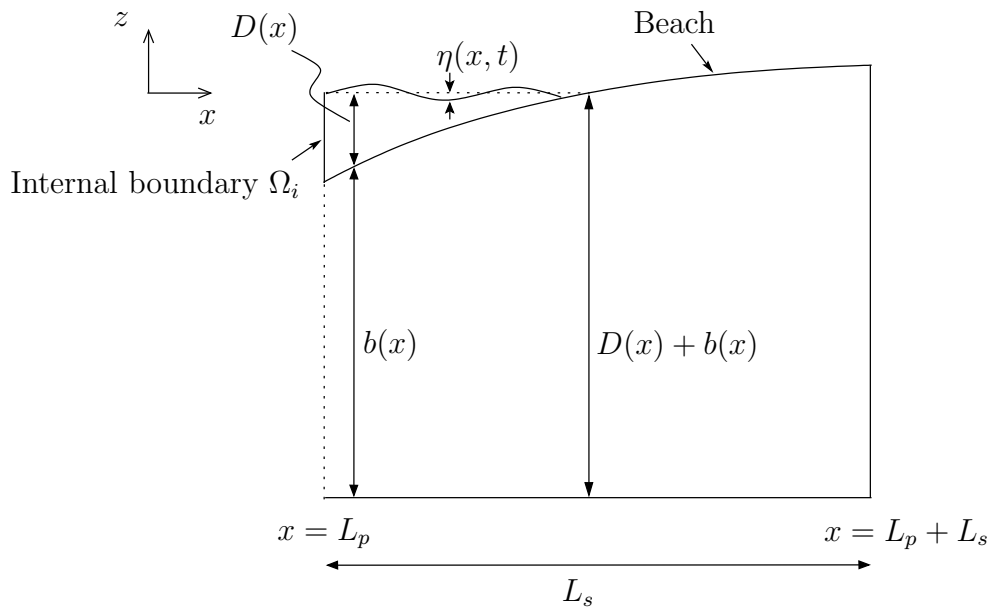


Figure 5: Shallow water domain (domain II)

The dimensional equations (2.22)-(2.23) are scaled using the following scalings:

$$u = Uu', \quad x = L_s x', \quad t = \frac{L_s}{U} t', \quad h = Hh', \quad b = Hb' \quad \text{and} \quad g = g' \frac{U^2}{H},$$

where U is the velocity scale, L_s the horizontal scale and H the vertical scale. The dimensionless quasi-linear formulation of the shallow water equations in one spatial dimension then read as:

$$\frac{\partial u'}{\partial t'} + u' \frac{\partial u'}{\partial x'} + g' \frac{\partial h'}{\partial x'} = -g' \frac{\partial b'}{\partial x'}, \quad (2.24)$$

$$\frac{\partial h'}{\partial t'} + \frac{\partial(h'u')}{\partial x'} = 0, \quad (2.25)$$

The dimensionless quasi-linear formulation (2.24)-(2.25) can be written in a form, conservative for \mathbf{u} ,

$$\frac{\partial \mathbf{u}}{\partial t} + \mathbf{u} \frac{\partial f(\mathbf{u})}{\partial x} = S \quad (2.26)$$

with $\mathbf{u} = (hu, h)^T$ and $S = (-gh \frac{\partial b}{\partial x}, 0)^T$, topographic term S , and transpose $(\cdot, \cdot)^T$

2.3.1 Variational formulation

The Lagrangian functional of the non-linear 1D shallow water equations is given as:

$$\mathcal{L}(\phi, h) = \int_{t_0}^{t_1} \int_{L_p}^{L_p+L_s} \left\{ \left(\frac{1}{2} h (\partial_x \phi)^2 + \frac{1}{2} g ((h+b)^2 - b^2) \right) - \phi \partial_t h \right\} dx dt, \quad (2.27)$$

with $\phi = \phi(x, t)$, $h = h(x, t)$, $b = b(x)$ and L the length of the domain in the x direction.

The equations of motion can be obtained using the first variation around ϕ and h :

$$\delta \mathcal{L}(\phi + \varepsilon \delta \phi, h + \varepsilon \delta h) = \frac{d}{d\varepsilon} \mathcal{L}(\phi + \varepsilon \delta \phi, h + \varepsilon \delta h) \Big|_{\varepsilon=0} = 0, \quad \text{and} \quad (2.28)$$

Writing (2.28) out:

$$\begin{aligned}
\delta\mathcal{L}(\phi + \varepsilon\delta\phi, h + \varepsilon\delta h) &= \frac{d}{d\varepsilon}\mathcal{L}(\phi + \varepsilon\delta\phi, h + \varepsilon\delta h)\Big|_{\varepsilon=0} = \\
&= \frac{d}{d\varepsilon} \int_{t_0}^{t_1} \int_{L_p}^{L_p+L_s} \left\{ \frac{1}{2}(h + \varepsilon\delta h)(\partial_x(\phi + \varepsilon\delta\phi))^2 + \frac{1}{2}g((h + \varepsilon\delta h + b)^2 - b^2) + \right. \\
&\quad \left. - (\phi + \varepsilon\delta\phi)\partial_t(h + \varepsilon\delta h) \right\} dx dt \Big|_{\varepsilon=0} = \\
&= \frac{d}{d\varepsilon} \int_{t_0}^{t_1} \int_{L_p}^{L_p+L_s} \left\{ \frac{1}{2}(h + \varepsilon\delta h) \left((\partial_x\phi)^2 + 2\varepsilon\partial_x\phi\partial_x(\delta\phi) + \varepsilon^2(\partial_x(\delta\phi))^2 \right) + \right. \\
&\quad + \frac{1}{2}g(h^2 + 2\varepsilon h\delta h + 2hb + 2\varepsilon b\delta h + \varepsilon^2(\delta h)^2 + b^2 - b^2) + \\
&\quad \left. - \phi\partial_t h - \varepsilon\phi\partial_t(\delta h) - \varepsilon\delta\phi\partial_t h - \varepsilon^2\delta\phi\partial_t(\delta h) \right\} dx dt \Big|_{\varepsilon=0} = \\
&= \frac{d}{d\varepsilon} \int_{t_0}^{t_1} \int_{L_p}^{L_p+L_s} \left\{ \frac{1}{2} \left(h(\partial_x\phi)^2 + 2\varepsilon h\partial_x\phi\partial_x(\delta\phi) + h\varepsilon^2(\partial_x(\delta\phi))^2 + \varepsilon\delta h(\partial_x\phi)^2 + 2\varepsilon^2\delta h\partial_x\phi\partial_x(\delta\phi) + \right. \right. \\
&\quad \left. \left. + \varepsilon^3\delta h(\partial_x(\delta\phi))^2 \right) + \frac{1}{2}g(h^2 + 2\varepsilon h\delta h + 2hb + 2\varepsilon b\delta h + \varepsilon^2(\delta h)^2) + \right. \\
&\quad \left. - (\phi\partial_t h + \varepsilon\phi\partial_t(\delta h) + \varepsilon\delta\phi\partial_t h + \varepsilon^2\delta\phi\partial_t(\delta h)) \right\} dx dt \Big|_{\varepsilon=0} = \\
&= \int_{t_0}^{t_1} \int_{L_p}^{L_p+L_s} \left\{ \frac{1}{2} \left(2h\partial_x\phi\partial_x(\delta\phi) + \delta h(\partial_x\phi)^2 \right) + \frac{1}{2} \left(2h\delta h + 2b\delta h \right) - \phi\partial_t(\delta h) - \delta\phi\partial_t h \right\} dx dt = \\
&= \int_{t_0}^{t_1} \left[h\partial_x\phi\delta\phi \right]_{L_p}^{L_p+L_s} dt + \int_{L_p}^{L_p+L_s} \left[-\phi\delta h \right]_{t_0}^{t_1} dx + \\
&\quad + \int_{t_0}^{t_1} \int_{L_p}^{L_p+L_s} ss \left\{ (\delta h)\partial_t\phi - \delta\phi\partial_t h + \frac{1}{2}\delta h(\partial_x\phi)^2 + gh\delta h + gb\delta h - \partial_x(h\partial_x\phi)(\delta\phi) \right\} dx dt = \\
&= \int_{t_0}^{t_1} \left[h\partial_x\phi\delta\phi \right]_{L_p}^{L_p+L_s} dt + \int_{L_p}^{L_p+L_s} \left[-\phi\delta h \right]_{t_0}^{t_1} dx + \\
&\quad + \int_{t_0}^{t_1} \int_{L_p}^{L_p+L_s} \left\{ (\delta h)(\partial_t\phi + \frac{1}{2}(\partial_x\phi)^2 + gh + gb) + (\delta\phi)(-\partial_t h - \partial_x(h\partial_x\phi)) \right\} dx dt = 0
\end{aligned} \tag{2.29}$$

Because we are considering only domain II in this paragraph, the internal boundary $\partial\Omega_i$ is taken to be a fixed wall. Then because δh and $\delta\phi$ are zero at $x = L_p$, $x = L_p + L_s$, $t = t_0$, $t = t_1$ and because of the arbitrariness of δh and $\delta\phi$, this results in:

$$\begin{aligned}
\partial_t\phi + \frac{1}{2}(\partial_x\phi)^2 + g(h + b) &= 0 \\
-\partial_t h - \partial_x(h\partial_x\phi) &= 0.
\end{aligned}$$

Integrating the first equation with respect to x and substituting $\partial_x\phi = u$ this becomes:

$$\partial_t u + \partial_x \left(\frac{1}{2}u^2 + g(h + b) \right) = 0 \tag{2.30a}$$

$$\partial_t h + \partial_x(hu) = 0. \quad (2.30b)$$

2.4 Coupling of the models

The shallow water model and the potential flow model have to be coupled in such a way that the information is passed correctly from one domain into the other. The coupling is accomplished by specifying boundary conditions for each model at the internal boundary between the two domains. In order to determine the internal boundary conditions for each model, the functional for the whole domain is considered. This functional can be obtained by adding the functional of the linear potential flow model and the non-linear shallow water model on the corresponding domains:

$$\begin{aligned} \mathcal{L}(\Phi, \phi, \eta, h) = & \int_{t_0}^{t_1} \int_{\Omega} -\frac{1}{2} |\nabla \Phi|^2 \, dx \, dz \, dt + \int_{t_0}^{t_1} \int_{\partial \Omega_s} \left\{ -\frac{1}{2} g \eta^2 + \Phi \partial_t \eta \right\} \, dx \, dt + \\ & + \int_{t_0}^{t_1} \int_{L_p}^{L_p+L_s} \left\{ \left(\frac{1}{2} h (\partial_x \phi)^2 + \frac{1}{2} g ((h+b)^2 - b^2) \right) - \phi \partial_t h \right\} \, dx \, dt. \end{aligned} \quad (2.31)$$

The equations of motion can again be obtained by determining the critical point(s) of the Lagrangian using the first variation around Φ , ϕ , η and h . This results in:

$$\begin{aligned} & \int_{t_0}^{t_1} \int_{\Omega} (\delta \Phi) (\nabla^2 \Phi) \, dx \, dz \, dt + \int_{t_0}^{t_1} \int_{\partial \Omega_s} (\delta \eta) (-\partial_t \Phi - g \eta) + (\delta \Phi) (\partial_t \eta - \nabla \Phi \cdot n_s) \, dx \, dt + \int_{\partial \Omega_s} \left[\Phi \delta \eta \right]_{t_0}^{t_1} \, dx + \\ & + \int_{t_0}^{t_1} \int_{\partial \Omega_b} (\delta \Phi) (-\partial_x \Phi) \, dx \, dz \, dt + \int_{t_0}^{t_1} \int_{\partial \Omega_l} (\delta \Phi) (\partial_x \Phi) \, dz \, dt + \int_{t_0}^{t_1} \int_{\partial \Omega_r} (\delta \Phi) (-\partial_x \Phi) \, dz \, dt + \\ & + \int_{t_0}^{t_1} \int_{\partial \Omega_{b2}} (\delta \Phi) (-\nabla \Phi \cdot n_{b2}) \, dz \, dt + \int_{t_0}^{t_1} \int_{\partial \Omega_i} (\delta \Phi) (-\partial_x \Phi) \, dz \, dt + \int_{t_0}^{t_1} \left[h \partial_x \phi \delta \phi \right]_{L_p}^{L_p+L_s} \, dt + \\ & + \int_{L_p}^{L_p+L_s} \left[-\phi \delta h \right]_{t_0}^{t_1} \, dx + \int_{t_0}^{t_1} \int_{\Omega} \left\{ (\delta h) (\partial_t \phi + \frac{1}{2} (\partial_x \phi)^2 + gh + gb) + (\delta \phi) (-\partial_t h - \partial_x (h \partial_x \phi)) \right\} \, dx \, dt = 0 \end{aligned} \quad (2.32)$$

Because of the arbitrariness of the variations and the fact that the variations are zero at the boundaries excluded $\partial \Omega_i$, this reduces to:

$$\begin{aligned} & \nabla^2 \Phi = 0 \text{ on } \Omega, \\ & -\partial_t \Phi - g \eta = 0 \text{ and } \partial_t \eta - \nabla \Phi \cdot n_s = 0 \text{ on } \partial \Omega_s, \\ & \partial_z \Phi = 0 \text{ on } \partial \Omega_b, \\ & \partial_x \Phi = 0 \text{ on } \partial \Omega_l, \\ & -\partial_x \Phi = 0 \text{ on } \partial \Omega_r, \\ & -\nabla \Phi \cdot n_{b2} = 0 \text{ on } \partial \Omega_{b2}, \\ & \int_{t_0}^{t_1} \left[h \partial_x \phi \delta \phi \right]_{L_p}^{L_p+L_s} \, dt = - \int_{t_0}^{t_1} \int_{\partial \Omega_i} (\delta \Phi) (\partial_x \Phi) \, dz \, dt \text{ on } \partial \Omega_i, \\ & \partial_t u + \partial_x \left(\frac{1}{2} u^2 + g(h+b) \right) = 0 \text{ on domain II}, \\ & \partial_t h + \partial_x (hu) = 0 \text{ on domain II}. \end{aligned}$$

The boundary integral on $\partial\Omega_i$ can be written as:

$$-h \int_{t_0}^{t_1} \partial_x \phi \delta \phi \Big|_{x=L_p} dt = - \int_{t_0}^{t_1} \int_{\partial\Omega_i} (\delta\Phi)(\partial_x\Phi) dz dt \text{ on } \partial\Omega_i. \quad (2.33)$$

or

$$h \partial_x \phi \delta \phi \Big|_{x=L_p} = \int_{\partial\Omega_i} (\partial_x\Phi)(\delta\Phi) dz \text{ on } \partial\Omega_i. \quad (2.34)$$

Because the depth-averaged shallow water equations are considered, the velocity potential $\phi(x, t)$ represents the depth-averaged velocity potential:

$$\phi(x, t) = \bar{\Phi}(x, t) = \frac{1}{\eta(x) + D(x)} \int_{-D(x)}^{\eta(x)} \Phi(x, z, t) dz, \quad (2.35)$$

and also

$$\delta\phi(x, t) = \overline{\delta\Phi}(x, t) = \frac{1}{\eta(x) + D(x)} \int_{-D(x)}^{\eta(x)} \delta\Phi(x, z, t) dz. \quad (2.36)$$

The waterheight h for the shallow water model at the internal boundary equals $\eta(L_p) + D(L_p)$, so the left hand side of (2.34) becomes:

$$(\eta(L_p) + D(L_p)) \partial_x \bar{\Phi}(L_p, z, t) \overline{\delta\Phi}(L_p, z, t) = \quad (2.37)$$

$$= (\eta(L_p) + D(L_p)) \frac{1}{\eta(L_p) + D(L_p)} \partial_x \bar{\Phi}(L_p, z, t) \int_{-D(L_p)}^{\eta(L_p)} \delta\Phi(L_p, z, t) dz = \quad (2.38)$$

$$= \int_{-D(L_p)}^{\eta(L_p)} \partial_x \bar{\Phi}(L_p, z, t) \delta\Phi(L_p, z, t) dz. \quad (2.39)$$

In the linear potential flow model $\eta \approx 0$, so $D + \eta \approx D$. At the internal boundary $\partial\Omega_i$ we then have:

$$\int_{-D(L_p)}^0 \partial_x \bar{\Phi}(L_p, z, t) \delta\Phi(L_p, z, t) dz \quad (2.40)$$

Equation (2.34) then becomes:

$$\int_{-D(L_p)}^{\eta(L_p)} \partial_x \bar{\Phi}(L_p, z, t) \delta\Phi(L_p, z, t) dz = \int_{-D(L_p)}^0 \partial_x \bar{\Phi}(L_p, z, t) \delta\Phi(L_p, z, t) dz, \quad (2.41)$$

If $D + \eta$ is approximate by D for the shallow water model at the internal boundary, the above equation reduces to

$$\int_{-D(L_p)}^0 \partial_x \bar{\Phi}(L_p, z, t) \delta\Phi(L_p, z, t) dz = \int_{-D(L_p)}^0 \partial_x \Phi(L_p, z, t) \delta\Phi(L_p, z, t) dz, \quad (2.42)$$

or

$$\int_{-D(L_p)}^0 (\partial_x \bar{\Phi}(L_p, z, t) - \partial_x \Phi(L_p, z, t)) \delta \Phi(L_p, z, t) dz = 0. \quad (2.43)$$

Because of the arbitrariness of the variation, this reduces to the following condition at the internal boundary:

$$\partial_x \bar{\Phi}(L_p, z, t) - \partial_x \Phi(L_p, z, t) = 0 \quad (2.44)$$

$$\partial_x \bar{\Phi}(L_p, z, t) = \partial_x \Phi(L_p, z, t). \quad (2.45)$$

Meaning that the depth-averaged velocity of the shallow water model and the velocity of the potential flow model have to be equal at the internal boundary.

2.5 Conclusion

Conclusion(s) of chapter 2.

3 Numerical methods

3.1 Introduction

In this chapter the numerical methods for solving the potential flow model (section 3.2) and the shallow water equations (section 3.3) are presented. The chapter ends with a comparison between the numerical solutions and the analytical solutions.

3.2 Linear potential flow model

The potential flow model is solved using a space discontinuous Galerkin method. The time integration is handled by an implicit time integration method (which one exactly, details?). In the next subsections numerical solutions of the linear potential flow model are compared with exact solutions for the case of harmonic waves without a wave maker and linear waves generated by a wave maker.

3.2.1 Harmonic waves

- Flat bottom.
- Dispersion, dissipation error.
- Initial condition.
- Comparison between analytical and numerical solutions.
- Give table of errors.

3.2.2 Linear waves generated by a wave maker

Exact solutions for the case where linear waves are generated by a wave maker can be formulated for a domain with a flat bottom (so no wave absorber present). Consider a domain $\Omega = [0, 1] \times [-H, 0]$ with the wave maker located at $x = 0$ and solid walls at the bottom and right boundary. A flap-type wave maker (see section 2.2) over the whole wall is considered, with the center of rotation located at $z = -H$, so $d = 0$ and $l = H$. This case is represented by the following set of equations:

$$\nabla^2 \Phi = 0 \quad \text{in } \Omega, \quad (3.1)$$

$$-\partial_t \Phi - g\eta = 0 \quad \text{at } z = 0, \quad (3.2)$$

$$\partial_t \eta - \nabla \Phi \cdot n_s = 0 \quad \text{at } z = 0, \quad (3.3)$$

$$\partial_z \Phi = 0 \quad \text{at } z = -H, \quad (3.4)$$

$$\partial_x \Phi = g(z)T(t) \quad \text{at } x = 0, \quad (3.5)$$

$$-\partial_x \Phi = 0 \quad \text{at } x = 1. \quad (3.6)$$

The general solution of the set of equations above for a harmonic oscillating wave board, i.e. with $T(t)$ as:

$$T(t) = i\bar{a}e^{-i\omega t}, \quad (3.7)$$

is given by (Westhuis p 87):

$$\Phi(x, z, t) = \frac{\bar{a}g}{\omega} \sum_{j=0}^{\infty} C_j \frac{\cosh(k_j(z + H))}{\cosh(k_j H)} e^{i(k_j x - \omega t)} \quad (3.8)$$

$$\eta(z, t) = \bar{a} \sum_{j=1}^{\infty} C_j e^{i(k_j x - \omega t)} \quad (3.9)$$

3.3 Shallow water model

The waves in the shallow water domain are described by the shallow water equations. The one dimensional shallow water equations in conservative form are stated as (see (2.26)):

$$\frac{\partial \mathbf{u}}{\partial t} + u \frac{\partial \mathbf{f}(\mathbf{u})}{\partial x} = S, \quad (3.10)$$

with

$$\mathbf{u} = \begin{pmatrix} hu \\ h \end{pmatrix} \quad \mathbf{f}(\mathbf{u}) = \begin{pmatrix} hu^2 + \frac{1}{2}gh^2 \\ hu \end{pmatrix},$$

and the topographic term S being:

$$S = \begin{pmatrix} -gh \frac{\partial b}{\partial x} \\ 0 \end{pmatrix}.$$

The above equations are discretized using a Godunov finite volume scheme. In order to handle flooding and drying correctly, the discretization of the shallow water equations according to Audusse et al. (2004) is applied, which is as follows:

$$\mathbf{U}_k^{n+1} = \mathbf{U}_k^n - \frac{\Delta t}{h_k} \left(\mathbf{F}_{k+\frac{1}{2}}(\mathbf{U}_{(k+\frac{1}{2})-}^n, \mathbf{U}_{(k+\frac{1}{2})+}^n) - \mathbf{F}_{k-\frac{1}{2}}(\mathbf{U}_{(k-\frac{1}{2})-}^n, \mathbf{U}_{(k-\frac{1}{2})+}^n) \right) + \frac{\Delta t}{h_k} S_k, \quad (3.11)$$

with the topographic term

$$S_k = \frac{1}{2}gh_{(k+\frac{1}{2})-}^2 - \frac{1}{2}gh_{(k-\frac{1}{2})+}^2, \quad (3.12)$$

$$\mathbf{U}_{(k-\frac{1}{2})-}^n = \begin{pmatrix} h_{(k+\frac{1}{2})-} u_k \\ h_{(k+\frac{1}{2})-} \end{pmatrix} \quad \text{and} \quad \mathbf{U}_{(k-\frac{1}{2})+}^n = \begin{pmatrix} h_{(k+\frac{1}{2})+} u_{k+1} \\ h_{(k+\frac{1}{2})+} \end{pmatrix}. \quad (3.13)$$

To ensure that the waterdepths $h_{(k+\frac{1}{2})-}$ and $h_{(k+\frac{1}{2})+}$ are non-negative, they are chosen as follows:

$$h_{(k+\frac{1}{2})-} = \max(h_k + b_k - b_{k+\frac{1}{2}}, 0), \quad h_{(k+\frac{1}{2})+} = \max(h_{k+1} + b_{k+1} - b_{k+\frac{1}{2}}, 0), \quad \text{with} \quad (3.14)$$

$$b_{k+\frac{1}{2}} = \max(b_k, b_{k+1}).$$

The HLL flux is used as a numerical flux, which is stated as:

$$\mathbf{F}_{k+\frac{1}{2}}^{hll} = \begin{cases} \mathbf{F}_L & \text{if } 0 < S_L, \\ \frac{S_R \mathbf{F}_L - S_L \mathbf{F}_R + S_L S_R (U_R - U_L)}{S_R - S_L} & \text{if } S_L \leq 0 \leq S_R, \\ \mathbf{F}_R & \text{if } 0 > S_R. \end{cases} \quad (3.15)$$

The wave speeds S_L and S_R are approximated as the smallest respectively the largest eigenvalue at the corresponding node.

To ensure stability of this explicit scheme, a CFL stability condition per cell is used for all eigenvalues λ_p at each \mathbf{U}_j^n :

$$\left| \frac{\Delta t}{h_k} \lambda_p(\mathbf{U}_k^n) \right| \leq 1, \quad (3.16)$$

where h_k is the cell width of cell k .

3.3.1 Riemann problem

The Riemann problem consists of a conservation law, in this case hyperbolic partial differential equations, together with piecewise constant data. It is therefore defined as

$$\mathbf{u}_t + \mathbf{f}_x = 0 \quad (3.17)$$

with a flux $\mathbf{f} = \mathbf{f}(\mathbf{u})$ and initial conditions

$$\mathbf{u}(x, t_0) = \begin{cases} \mathbf{u}_l & \text{if } x < x_0 \\ \mathbf{u}_r & \text{if } x > x_0 \end{cases}. \quad (3.18)$$

For the shallow water equations four types of solutions are considered:

- left shock wave, right shock wave
- left rarefaction wave, right shock wave
- left shock wave, right rarefaction wave
- left rarefaction wave, right rarefaction wave. The characteristics of each of these cases are depicted in figure ???.

For these cases exact solutions can be obtained (see Appendix ??? for the derivations), which makes comparison to the numerical solutions possible. In figures ??? the exact solutions are plotted against the numerical solutions on different times, for all of the four cases. As can be seen, there is some smearing at the discontinuities.

3.3.2 Burgers' solution

The shallow water equations with the topography term S equal to zero take the form of the Burger' equation $\partial_t q + q \partial_x q = 0$, when one of its Riemann invariants is taken to be constant as $u + 2\sqrt{gh} = c$, with $q(t, x) = c - 3\sqrt{gh}$.

The shallow water equations actually reduce to the Burgers' equation by choosing certain initial conditions:

The exact solution of the Burgers' equation is gives as:

...

A comparison between the exact and numerical solution for the Burgers' equation can be seen in figure ???.

3.4 Coupling of the models

The potential flow code and the shallow water code are ran sequentially. The information between the codes is exchanged through boundary conditions at the internal boundary. The shallow water code needs a velocity u and a waterheight h from the potential flow code. The potential flow code needs only a velocity u from the shallow water code. The algorithm of the combined codes is described in the flow chart in figure 6. At first the mesh of the whole domain is generated. After this both codes are initialized. In the next step the average velocity $u = \Phi_x$ and the waterheight h at the internal boundary of the potential flow part are computed. These values are necessary to check if the CFL condition is satisfied. If not, the time step is adjusted. Subsequently solutions of the shallow water are calculated at the new time step $n + 1$, with the water height h and $u = \Phi_x$ the average velocity at time step n as input. Next, solutions of the potential flow code are calculated at time step $n + 1$, with only the velocity u from the shallow water code at time step n as an input.

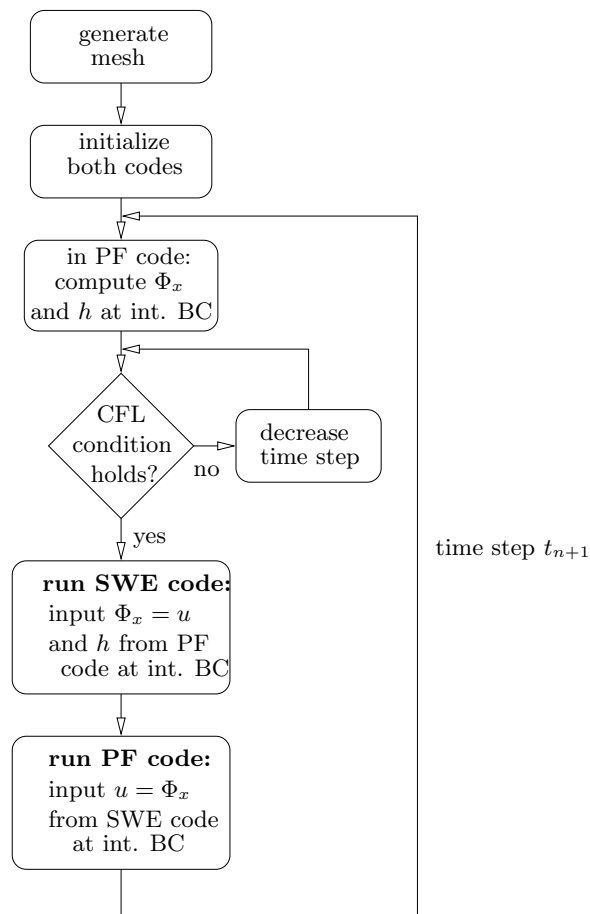


Figure 6: Flow chart of the coupled codes

3.4.1 Verification

The coupled model is verified by comparing numerical results with exact solutions. Exact solutions can be obtained for the following situation where there is a flat bottom for the PF

and SWE domain (see figure 7).

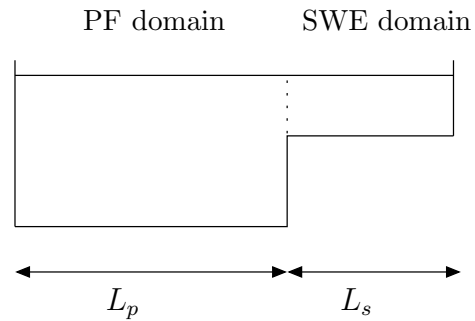


Figure 7: Domain for comparison with exact solutions

- Formulate exact solutions.
- Give plots with exact solutions and numerical solutions.
- Give table with errors for different grid sizes.

3.5 Conclusion

4 Experimental validation

4.1 Introduction

In this chapter the coupled linear potential and shallow water equations model is validated with experimental data from the Offshore Basin at MARIN.

4.2 Experimental data

- Describe setup of the Offshore Basin.
- Describe format of available data.
- Compare measurements with target wave patterns.

4.3 Numerical simulation

An exponential distribution of the elements in depth is applied for the potential flow model. For this, a transformation is used that transforms a uniform grid into a grid that decreases exponentially with decreasing depth. This transformation holds for a grid pictured in figure 8 and is stated as:

$$\bar{z} = \frac{\log\left(\frac{z-\beta}{h-1}\right)}{\log\left(\frac{0-1}{h-1}\right)}, \quad (4.1)$$

with $h \leq 0$. Increasing β results in more clustering near the top of the domain.

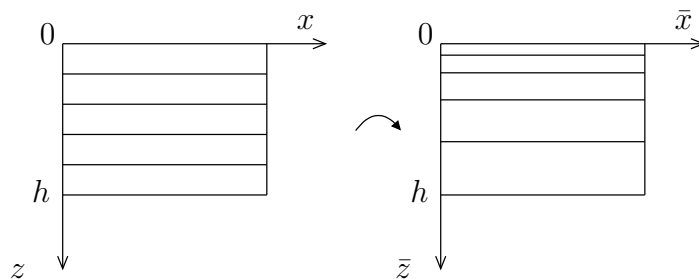


Figure 8: Transformation

- Describe scaling.
- Effect of location of internal boundary.

4.4 Conclusion

Conclusion(s) of chapter 4.

5 Conclusions and recommendations

5.1 Introduction

Introduction of chapter 6.

5.2 Conclusions

Conclusion(s) of the report.

5.2.1 Recommendations for MARIN

Recommendations for wave dampening in the offshore basin at MARIN.

5.2.2 Future research

Recommendations for future research with respect to the research done in this report.